Electrical and thermal properties of bisphenol A propoxylate diglycidyl ether–piperazine copolymer/functionalized MWCNT composites

SERPIL YILMAZ, MUSTAFA ERSIN PEKDEMIR and MEHMET COŞKUN*

University of Fırat, Faculty of Science, Department of Chemistry, 23119 Elazığ, Turkey

Abstract: In this work, bisphenol A propoxylate diglycidyl ether–piperazine copolymer functionalized MWCNTs (oxidized MWCNT + aminated MWCNT) composites were prepared and structurally characterized using FTIR and NMR spectroscopy. The composites were investigated in terms of their electrical and thermal properties. The surface morphology of the composites was examined by SEM. It was observed that thermal stability decreased while the ac conductivity and dielectric constant (relative permittivity) increased with increasing functionalized MWCNT content (2, 5, 10 and 15 mass %) of the composites. The electrical conductivity increased with increasing temperature and the activation energy of ac conductivity was determined and discussed.

Keywords: bisphenol A; piperazine; MWCNT; composite; copolymer.

INTRODUCTION

Carbon nanotubes (CNTs), discovered by Iijima,[1] have remarkable properties, such as mechanical properties, chemical stability, and electrical and thermal conductivity. They have received much attention for their many potential application, such as nanoelectronic and photovoltaic devices,[2,3] superconductors,[4] electromechanical actuators,[5] electrochemical capacitors,[6] nanowires[7] and nanocomposite materials.[8,9]

Polymer/CNT composites have attracted considerable attention owing to their unique mechanical, surface and multi-functional properties, and, resulting from their nano structure, an extremely large interfacial area between the CNT and the polymer matrix. After the publication of Iijima's report[1] on CNTs in 1991, many research articles and reviews on CNTs and their composites have been published.[10–15] In current years, many polymers, such as poly(methyl methacrylate) (PMMA), epoxy type polymers, poly(vinyl chloride) (PVC),

---

poly(vinyl alcohol) (PVA), polyethylene (PE), polystyrene (PS),[10] poly(glycidyl methacrylate) (PGMA),[16] poly(vinylidene fluoride) (PVF),[17] have been used widely as matrices for the preparation of polymer/CNT composites. There are reports in the literature on composites of epoxy-based polymers with CNTs. The mechanical properties of bisphenol A diglycidyl ether type epoxy resin were investigated by the addition of polyether polyol and amine functionalized multiwall carbon nano tube (MWCNT).[18] Curran *et al.*[19] have studied extensively the electrical properties of poly(bisphenol A carbonate) doped with MWCNTs. Particularly, the conductivity of both acid-treatment and pristine MWCNTs have been examined at different weight percents of nanotubes.

In the present study, a copolymer of bisphenol propoxylate diglycidyl ether (BPPDGE) with piperazine (P) was prepared. This condensation copolymer contains functional groups in its main chain, such as ether, hydroxyl, amine groups, aromatic rings, with epoxide groups at the chain ends. It was synthesized with the thought that a copolymer with these functional groups and its MWCNT composites may exhibit attractive electrical and thermal properties. In the investigated polymer, there are amine groups that could easily be interacted with oxidized MWCNT, and there are the ether groups that could easily be interacted with aminated MWCNT. For these reasons, MWCNTs containing two different functional groups were used together. Composites of this copolymer, poly-(BPPDGE-*co*-P), with the mixture of oxidized MWCNT and aminated MWCNT were studied for the first time in terms of electrical, thermal and surface properties. The effects of the mixture of oxidized MWCNT and aminated MWCNT on the properties of the composite were investigated.

EXPERIMENTAL

Materials

Toluene, ethanol, (3-aminopropyl)trimethoxysilane (3-APTMS) (99 %), 1,4-dioxane, tetrahydrofuran and bisphenol A propoxylate diglycidyl ether (M.W. 456.6 g mol^{-1}, PO/phenol, PO: propylene oxide) were obtained from Sigma–Aldrich and used without any purification. Piperazine was obtained from Sigma–Aldrich and recrystallized from diethyl ether before use. Multi-wall carbon nanotube (MWCNT, average diameter 9.5 nm, length >1.5 μm and purity > 95 %) was purchased from the Grafen Chemical Co.

Synthesis of oxidized MWCNT

Carboxyl-functionalized MWCNTs (oxidized MWCNT) were prepared by oxidation of MWCNTs in a mixture of concentrated HNO_3 and H_2SO_4 in a 1:3 ratio (by volume).

The procedure: MWCNT (2 g) and 40 mL of the acid mixture were added into a 250 mL flask equipped with a condenser, and the mixture was stirred vigorously. The flask was then immersed in an ultrasonic bath at room temperature for 20 min. The stirring of the mixture was continued under reflux for 10 h in an ultrasonic bath. The mixture was allowed to cool at room temperature and was then diluted with 250 mL of water, followed by neutralization with concentrated NaOH and then filtered. The residue was washed with water several times, washed with tetrahydrofuran (THF) to remove the water, and then dried under vacuum for 24 h at 50 °C.

Synthesis of MWCNTCOOSi(OCH$_3$)$_2$-n-propyl-NH$_2$

For silanization according to a method modified from literature,[20,21] 0.5 g of oxidized MWCNT was dispersed in an ultrasonic bath in 40 mL toluene for 15 min and then 2 g (3-aminopropyl)trimethoxysilane (3-APTMS) was added to the mixture. The mixture was refluxed for 6 h, and after cooling to room temperature, the product, MWCNTCOOSi(OCH$_3$)$_2$-*n*-propyl-NH$_2$ (aminated MWCNT), was separated by filtration, washed a few times with ethanol, and dried under vacuum at 50 °C for 24 h.

Copolymerization of bisphenol A propoxylate diglycidyl ether and piperazine

A method adapted from literature was used for the copolymerization.[22] Briefly, to a 25 mL flask containing 3.085 g (6.76 mmol) of bisphenol A propoxylate diglycidyl ether and 5 mL of 1,4-dioxane was added piperazine 0.5820 g (6.76 mmol recrystallized from diethyl ether) previously dissolved in 5 mL of 1,4-dioxane. After passing nitrogen gas through the resulting mixture, it was sonicated for 1 h and then refluxed on magnetic stirrer and heater for 3 days. At the end of this time, 0.55 g bisphenol A propoxylate diglycidyl ether dissolved in 2 mL 1,4-dioxane was added to the reaction flask and the refux was continued for 1 day more. The reaction content was then cooled to room temperature and diluted with about 20 mL of 1,4-dioxane. The polymer product, poly(BPPDGE-*co*-P), was precipitated by pouring the reaction mixture dropwise into an excess of methanol/water (1:1 by volume), filtered off and air-dried. The product was redissolved in 1,4-dioxane and reprecipitated in the same precipitator, filtered off and dried in vacuum oven at 50 °C for 24 h.

Preparation of the composites

For preparation of the composites, 0.45 g of the copolymer was dissolved in 5 mL of 1,4-dioxane. For preparing a composite containing 10 % by weight of functionalized MWCNT, 0.025 g of oxidized MWCNT and 0.025 g of aminated MWCNT were dissolved in 2 mL of 1,4-dioxane, and this mixture was added to the polymer solution. This mixture was stirred in an ultrasonic bath for 3 h, and then it was stirred using a magnetic stirrer at 80 °C for 1 h. Then, the mixture was cooled to room temperature, the composite was precipitated by adding the solution dropwise to a methanol–water mixture (1:1 v:v). The precipitate was filtered and dried under vacuum at 50 °C for 24 h. Finally, the composite was ground with an agate pestle and mortar to a very fine powder.

A series of BPPDGE-P copolymer/functional MWCNT composites containing 2, 5 and 15 mass % functionalized MWCNT were also prepared by a process similar to that described above.

Measurements

Infrared spectra were recorded on a Perkin–Elmer Spectrum One FTIR spectrometer, using KBr discs in the wavenumber range of 450 – 4000 cm^{-1}. Calorimetric measurements were realized on a Shimadzu DSC-50 thermal analyzer under a N$_2$ flow (100 mL/min) at a heating rate of 20 °C min^{-1}. Thermogravimetric analysis (TGA) studies were performed on a Shimadzu TGA-50 thermobalance under a dynamic N$_2$ atmosphere (flow rate 100 mL/min) at a heating rate of 10 °C min^{-1}.

For capacitance measurements according to a previous work,[23] the composite was ground with an agate pestle and mortar and the final fine powder was pressed at a pressure of four tons into disk-shaped samples. The thickness of the samples were 0.68 mm, 0.66, 0.64 and 0.65 for the composites containing 2 5, 10 and 15 mass % MWCNT, respectively. The surface area of all disks was 1.12 cm^2. The entire surface of the disk was coated with aluminum foil, which acts as a good contact for capacitance measurements.

The measurements were performed at room temperature with a QuadTech 7600 precision LRC meter impedance analyzer over the frequency range 0.1–2 kHz. The dielectric features against the frequency and temperature were examined. The ac conductivities of the composites against temperature were also examined at a constant frequency of 1 kHz.

A scanning electron microscope (SEM, Jeol JSM-700IF) was used to examine the distribution of nanoparticles in the composite materials. The powder samples were gold-coated before the measurements.

RESULTS AND DISCUSSION

Characterization of the matrix copolymer and the composites

The FTIR spectra of the mixture of oxidized MWCNT and aminated MWCNT, the matrix copolymer, poly(BPPDGE-*co*-P) and the composite containing 10 % of MWCNT mixture (oxidized MWCNT + aminated MWCNT) are shown in Fig. 1. In the spectrum presented in Fig. 1a, the O–H and C=O stretching vibrations of the carboxylic group of oxidized MWCNT are seen at 3440 and 1735 cm^{-1} (small peak), respectively. The broad peak at 1380 cm^{-1} and the broad band at 1600–1650 cm^{-1} may be assigned to O–H bending vibration (in addition to acidic O–H, probably O–H of atmospheric moisture on the surface)[21] and aromatic C=C stretching vibration (and also N–H in plane bending vibration)[24], respectively. The FTIR spectrum (a) also shows the characteristic bands at 3290 cm^{-1} (symmetric stretching vibration of N–H, the asymmetric vibration of N–H is under the band at 3440 cm^{-1}), 2925 and 2850 cm^{-1} (C–H stretching of CH$_2$ groups), bands at 1200–1000 cm^{-1} (Si–O–Si, Si–O–C and C–O stretching vibration) and 780 cm^{-1} (N–H out-of-plane bending vibration).

The FTIR spectrum of poly(BPPDGE-*co*-P) (Fig. 1b) shows characteristic peaks of the matrix copolymer. In this context, the six intense bands at 3430, 2970–2818, 1604, 1241, 1155–1000 and 827 cm^{-1} are the characteristic poly(BPPDGE-*co*-P) peaks that correspond to O–H stretching vibrations, aliphatic C––H stretching vibrations, aromatic C=C stretching vibrations, C(aromatic)–O–C (aliphatic) asymmetric stretching vibrations, aliphatic ether C–O–C, C–N stretching vibrations and *p*-disubstituted aromatic C–H out-of-plane bending vibrations, respectively. The bands at 3054, 1885 and 1764 cm^{-1}, 1365 and 1384 cm^{-1}, 913 and 740 cm^{-1} could be attributed to epoxide C–H and aromatic C–H stretching vibrations, overtone and combination bands of *p*-disubstituted aromatic, in plane bending vibrations of C(CH$_3$)$_2$ groups, epoxide symmetric ring stretching vibration and epoxide C–H bending vibration, respectively. The peaks corresponding to epoxide group (3054, 913 and 740 cm^{-1}) are weakened in the spectrum (Fig. 1c) of the composite (10 mass %), when compared to those of the matrix copolymer. This is probably due to the opening by the acid and amine groups of some parts of the epoxide ring.

The structure of the copolymer was confirmed by its ^{1}H-NMR spectrum (Fig. 2a), which shows characteristic signals. The signals at 7.12 and 6.76 ppm were
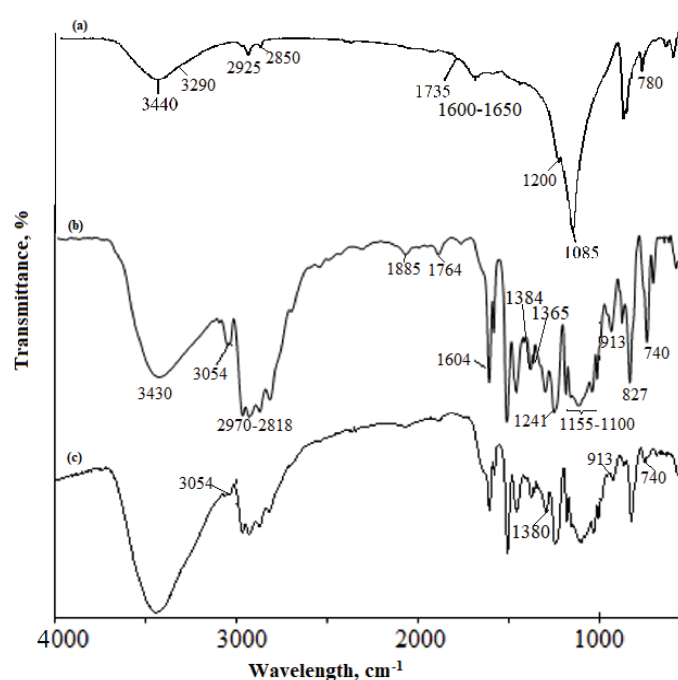
Fig. 1. FTIR spectra of: a) mixture of oxidized MWCNT and aminated MWCNT,
b) poly(BPPDGE-*co*-P) and c) the composite (10 mass %).

assigned to the aromatic protons *meta* and *ortho* to the oxygen atom, respectively. The signals between 3.25–4.7 ppm are due to CH and CH_2 protons bonded to oxygen, and the signals between 2.2–3.0 are due to epoxide ring protons and CH_2 protons bonded to nitrogen. Peaks between 1.0 and 2.0 ppm include methyl protons in the side chain of the aromatic ring and CH_2 protons not bonded to oxygen. All the assignments are shown in the copolymer formula in Fig. 2. The ^{13}C-NMR spectrum (Fig. 2b) shows characteristic signals for bisphenol A propoxylate diglycidyl ether at 156, 143, 128 and 114 ppm due to quaternary carbon (p) bonded to oxygen, quaternary carbon (q) bonded to aliphatic carbon, CH carbons in the *meta* and *ortho* position on the aromatic ring, respectively. The other assignments are shown in the copolymer formula in Fig. 2.

Figure 3 shows the SEM images of the copolymer (Fig. 3a), pristine MWCNT (Fig. 3b), MWCNT silanized with (3-aminopropyl)trimethoxysilane (aminated MWCNT, Fig. 3c) and the composite containing 15 mass % of the mixture of oxidized MWCNT and aminated MWCNT (Fig. 3d).

The SEM micrograph of the pure matrix copolymer suggests a smooth surface. A more homogeneous distribution of MWCNT is observed after silanization. In addition to this, the morphology of MWCNTs after functionalization is observed to have remained intact with minimal visible tube damage, which indi-
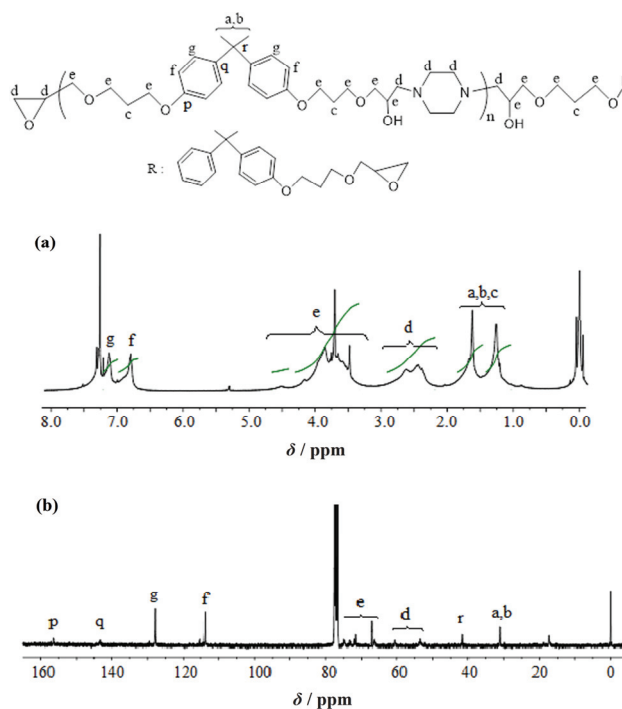
Fig. 2. a) ^{1}H-NMR and b) ^{13}C-NMR spectra of poly(BPPDGE-*co*-P) (solvent: CDCl$_3$).

cates that the MWCNTs are strong enough to withstand the functionalization process. SEM image of the composite prepared with the mixture of aminated MWCNT and oxidized MWCNT (Fig. 3d) was compared with that of the composite prepared with the unmodified MWCNT (Fig. 3e). It is seen that the composite prepared with the functional MWCNT particles are dispersed more homogeneously than that prepared with unmodified MWCNT in the polymer matrix. This is because the presence of the carboxylic groups and amino groups on the nanotube surface are likely to give strong interfacial interactions between the polymer matrix and the nanotubes in polymer composites.[25] That is, oxygen (–O–) in the epoxide of the end groups and oxygen in the ether groups of polymer main chain and –N– in the piperazine unit of the matrix copolymer may form hydrogen bonds with the –COOH and –NH$_2$ groups of the functionalized MWCNTs.

To obtain knowledge of the viscosity of poly(BPPDGE-*co*-P), the limiting viscosity number [η] was determined using the Huggins equation:

$$\frac{\eta_{sp}}{c} = [\eta] + k'[\eta]^2 c$$

Flow times of poly(BPPDGE-*co*-P) solutions with concentrations (*c*) between 0.556–0.280 g copolymer per dL chloroform and pure chloroform were

determined using an Ubbelohde viscometer. The Huggins line was obtained from plot of η_{sp}/c *vs. c*, where η_{sp} is the specific viscosity. From these measurements, the limiting viscosity number of the polymer in chloroform solution and the Huggins constant, *k'*, were obtained as 0.34 dL/g and 0.38 (generally $0.3 < k' < 0.4$) at 22 °C, respectively.
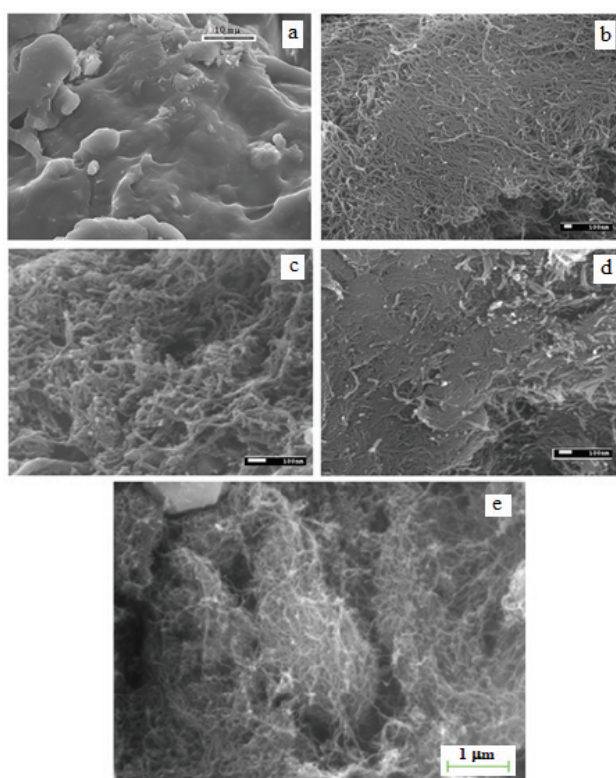

Fig. 3. SEM images of the matrix copolymer (a, 2000×), original MWCNT as received (b, 30000×), aminated MWCNT (c, 70000×), composite containing the mixture of aminated MWCNT and oxidized MWCNT (d, 15 mass %, 50000×) and the composite with unmodified MWCNT (e, 15 mass %, 45000×).

Electrical investigation

The dielectric constant*, which is one of the electrical properties of materials, is a measure of the influence of a particular dielectric on the capacitance of a condenser. When a dielectric is placed between two electric charges, it reduces the force acting between them, just as if they had been moved apart from each other. The dielectric constant of a material affects how electromagnetic signals

---

* Relative permittivity

move through the material. It is calculated from capacitance measurements using the following equation:

$$\varepsilon' = \frac{C_{\mathrm{p}} d}{\varepsilon_0 A}$$

where C_{p} is parallel capacitance, ε_0 is the permittivity in free space, d is thickness of sample material and A is surface area of the sample. In Fig. 4 are shown the dependence of the dielectric constant (Fig. 4a) and dielectric loss factor (Fig. 4b) on frequency (0.10–2.5 kHz) for all samples and on the percentage of functional MWCNT (Fig. 4c) in the composites. It can be distinctly observed that the dielectric constant and dielectric loss decrease with increasing frequency.
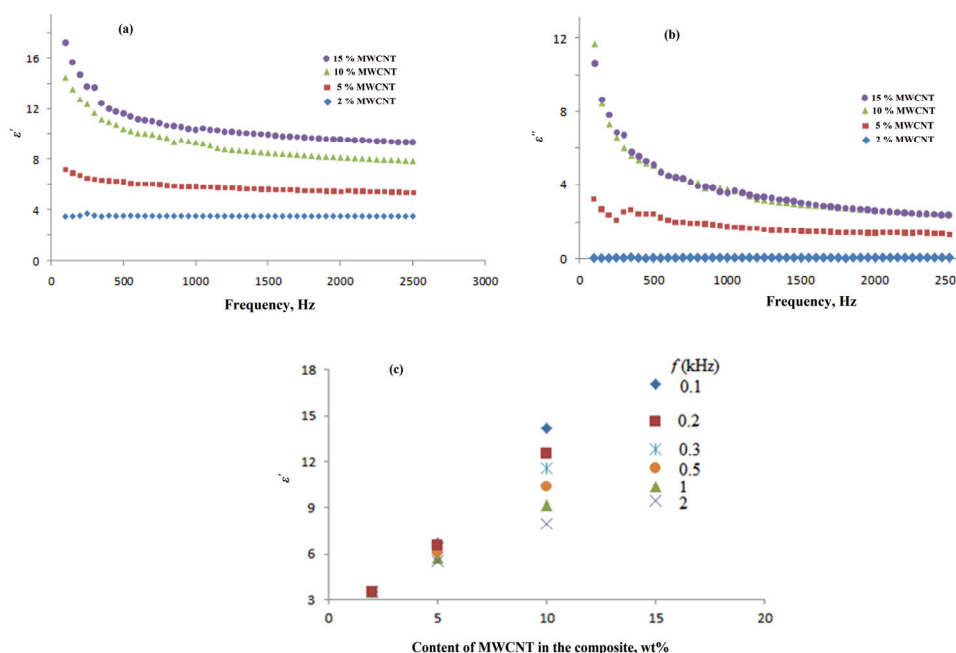

Fig. 4. Frequency dependencies of: a) dielectric constant (ε') and b) dielectric loss factor (ε''); c) the composite concentration dependence of dielectric constant at different frequencies.

As shown in the Fig. 4, for the composite containing 2 mass % modified MWCNTs, the dielectric constant remained approximately constant with increasing frequency from 0.1 to 2.5 kHz, while that of the composite containing 5 mass % modified MWCNTs decreased slightly. When the MWCNTs loading was 10 and 15 mass %, the dielectric constant of the composite decreased rapidly up to about 0.6 kHz after which the decline slowed down. A similar behavior was also observed previously, e.g., for calcium copper titanate/MWCNT/polyarylene ether nitrile composites,[25] for some ceramics[26] and poly(urethane)/poly(aniline)

composites.[27] The large value of the dielectric constant at a low frequency is due to the presence of electric polarization of polar groups. The decrease in the value of dielectric constant with frequency is because the frequency of the electric charge carriers cannot follow the alternation of the applied electric field beyond a certain critical frequency. The very low value of dielectric constant at higher frequencies is important for the fabrication of materials for ferroelectronic, photonic and electro-optic devices. Fig. 4b shows that the dielectric constant is more dependent on the frequency in the composites containing higher concentrations.

The changes in the dielectric constant (ε') with temperature for the composites at different concentration and at 1 kHz are shown in Fig. 5. With increasing temperature, the dielectric constant initially increases moderately from 320 to 340 K for the 15 mass % composite and from 320 to 360 K for the 10 mass % composite and thereafter, it increases rapidly up to 375 K for the 15 mass % composite and up to 390 K for the 10 mass % composite. For the 5 and 2 mass % composites, the dielectric constant increases slightly with increasing temperature from 320 to nearly 390 K and then increases rapidly up to 420 K for the 5 mass % composite and up to 430 K for the 2 mass % composite.
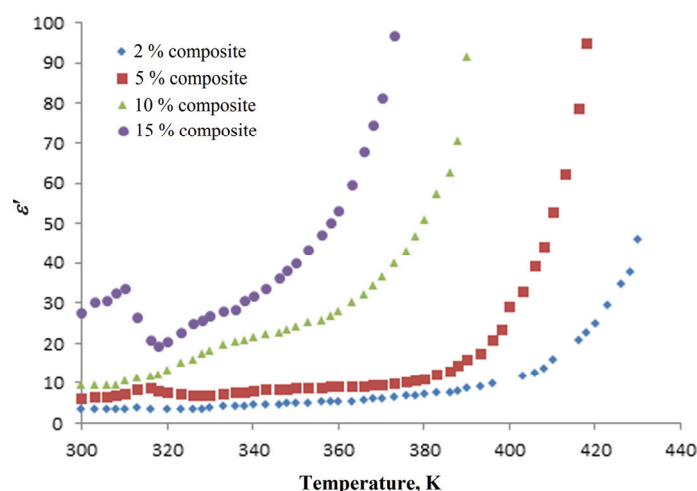

Fig. 5. Temperature dependence of dielectric constant of the composites at 1 kHz.

The variation in the ac conductivity with frequency and temperature at different modified MWCNT contents are shown in Fig. 6. The electrical conductivity (log σ) of the composites increases approximately linearly with increasing the applied frequency (log f, from 2 to 3.4, Fig. 6a), moderately for the 2 mass % composite and slowly for the other composites. The conductivity increases also with increasing MWCNT content in the composites.

The composite samples with increasing MWCNT content are thermally acti-vated by heating at higher temperature. The activation energy of the ac conduct-ivity was obtained using the Arrhenius equation:[28]

$$\sigma = \sigma_0 \exp\left(-E_a/k_b T\right)$$

where σ is the conductivity, σ_0 is the pre-exponential factor of conductivity, k_b is the Boltzmann constant, T is the temperature in Kelvin, and E_a is the activation energy. Plots of log σ *vs.* $1/T$ at 1 kHz are shown in Fig. 6b. The ac activation energies were calculated from the slopes in the linear region (range of 320–440 K) of the plots. It is clear from the plots that above ≈320 K, the ac conductivity increased with increasing temperature and increasing MWCNT content. The incorporation of the modified MWCNT increased the conductivity from 0.18×10^{-7} to 8.19×10^{-7} S cm^{-1} at 320 K and from 1.18×10^{-5} to 17.06×10^{-5} S cm^{-1} at 400 K when the filler content was increased from 2 to 15 mass %. The plot of log σ *vs.* $1/T$ indicated that the observed conductivity did not correspond to single thermally activated process and could not be described by a simple exp-onential relationship.[29] Thus, it could be concluded that the ac conductivity dep-ended on temperature and that it is reasonable to assume that a range of acti-vation energies were involved. The values of the activation energies are given in Table I.
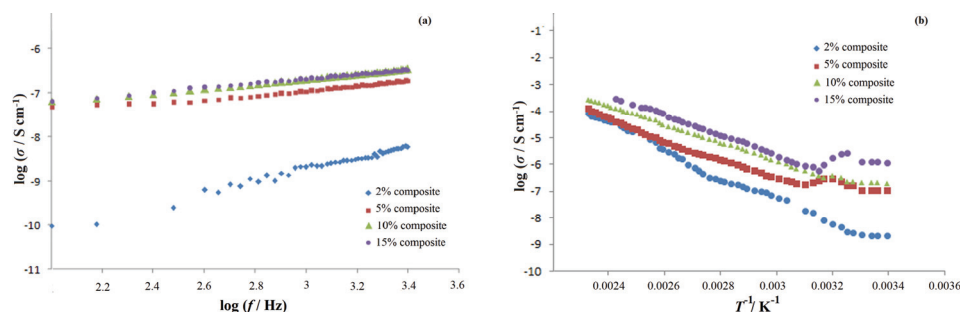

Fig. 6. Variation of ac conductivity with: a) frequency and b) temperature.

TABLE I. Activation energy of ac conductivity at 1 kHz

Composite	E_a / eV
2 mass % of modified MWCNT	0.396
5 mass % the modified MWCNT	0.335
10 mass % the modified MWCNT	0.327
15 mass % the modified MWCNT	0.312

As can be seen from Table I, the activation energy of ac conductivity dec-reased as the concentration of modified MWCNT increased. A similar trend for activation energy was observed for polyester/MWCNT composites[30] and carbon black/epoxy composites.[31] Similar to the comments in the literature,[30,31] deg-

rease in E_a values with the MWCNT content may be due to an increase of polarization energy and/or charge carrier density leading to a decrease of the domain boundary potential of MWCNT aggregate into the matrix polymer.

Since it was not possible to prepare a disc of the matrix copolymer, its electrical properties could not be measured.

Thermal investigation

Thermogravimetric curves of the copolymer, the mixture of oxidized MWCNT and aminated MWCNT and the composites are shown in Fig. 7. The initial decomposition temperatures (T_{IDT}), defined as the temperature at 5 % mass loss, for the copolymer, the mixture of oxidized MWCNT and aminated MWCNT and the composites (2, 5, 10 and 15 mass %) were 290, 298, 271, 268, 269 and 275 °C, respectively, as values obtained from the TG curves. These values showed that T_{IDT} shifted to lower values for all composites. This result shows that the mixture of oxidized MWCNT and aminated MWCNT decreased the thermal stability of nanocomposites according to the temperature at which the decomposition began. Probably, radicals that remained within the MWCNT during the oxidation initiated the decomposition of the polymer at a lower temperature.
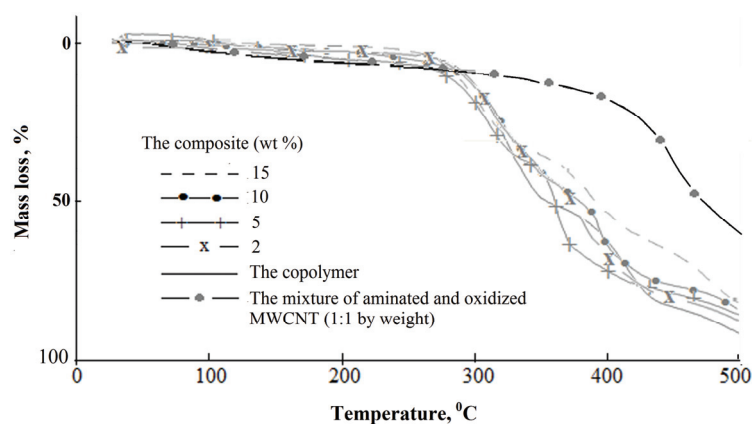

Fig. 7. The TG curves of the materials investigated in this study.

Furthermore, with increasing content of modified MWCNT in the composites, the residues at 500 °C increased from 10.8 to 18.3 mass %, while the matrix copolymer left a 8.3 mass % residue at 500 °C (Fig. 7). The thermal data are summarized in Table II. The original polymer and the composites showed three-stage decomposition curves. The residues at 350 °C were 51.5 mass % for the matrix copolymer, and 59.2, 61.0, 62.0 and 64 mass % for the composites containing 2, 5, 10 and 15 mass % modified MWCNT, respectively.

The DSC curves in Fig. 8 show that the matrix copolymer, poly(BPPDGE-
-*co*-P), had a glass transition temperature (T_g) of 152 °C, whereas the T_g values
of the composites containing 2, 5, 10 and 15 mass % MWCNT were 57, 54, 54
and 58 °C. The literature T_g value for poly(bisphenol A propoxylate diglycidyl
ether), poly(BPPDGE), was 125 °C.[32] The T_g value for the copolymer was
higher than that for poly(BPPDGE) due to the presence of rigid piperazine units
in the main chain of the former, which prevent chain mobility and lead to an inc-
rease of the free volume in the copolymer.

TABLE II. Some thermal properties of the materials investigated in this study

Material	$T_g{}^a$ °C	$T_{IDT}{}^b$ °C	$T_{secd}{}^c$ °C	$T_{trd}{}^d$ °C	Residue at 350 °C, mass %	Residue at 500 °C, mass %
The mixture of oxidized and aminated MWCNT	–	298	–	–	> 95	40.0
Poly(BPPDGE-*co*-P)	152	290	374	446	51.4	8.3
Composite: 2 mass %	57	271	363	449	59.2	10.8
5 mass %	54	268	349	447	61.0	14.2
10 mass %	54	269	391	465	62.0	15.8
15 mass %	58	275	364	454	64.2	18.3

[a]Glass transition temperature; [b]initial decomposition temperature defined as the temperature at a weight loss of
5 %; [c]the temperature at which the second decomposition stage begins; [d]the temperature at which the third
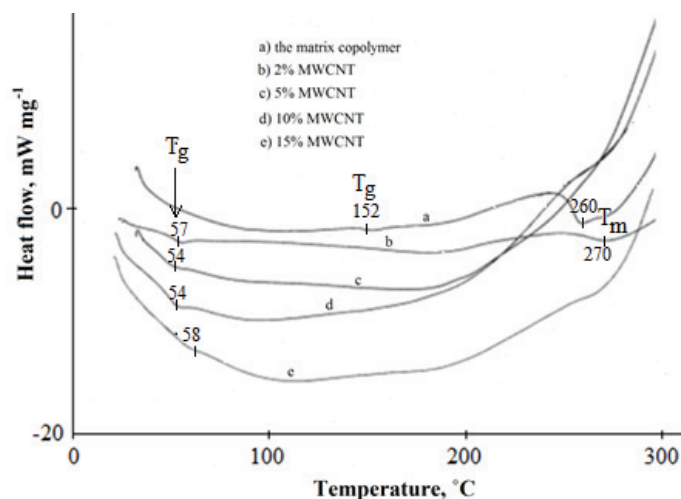decomposition stage begins

Fig. 8. The DSC curves of the matrix copolymer and the composites.

It is also interesting that the T_g values of the composites were very low com-
pared to that of the copolymer. The copolymer contains etheric groups, amine
groups and hydroxyl groups in its main chain, and epoxy end groups. Strong
dipole–dipole interactions and hydrogen bond interactions occur between these

groups along the chain. When MWCNT nanoparticles were introduced between the copolymer chains in the composites, these strong physical interactions were broken, and the chains were separated from one another, which means that the free volume in the polymer were increased and the T_g value decreased. It was reported that the addition of a monoamine with a long hydrocarbon chain or an aliphatic di-epoxy compound to EPON 826 polymer that bears epoxy end groups, and ether and OH groups in the main chain significantly reduced the T_g value of the polymer.[33]

While the matrix copolymer exhibited a melting point at about 260 °C, only the 2 mass % composite showed a melting point, at about 270 °C.

CONCLUSIONS

Composites were prepared from poly(BPPDGE-*co*-P) and a mixture of aminated MWCNT and oxidized MWCNT, and characterized by FTIR and NMR spectroscopy. Surface morphologies showed that homogenous composites were formed. The ac electrical conductivity, the dielectric constant, and the dielectric loss factor of the composites increased with the MWCNT concentration (2, 5, 10 and 15 mass %) in the composites. The increase in dielectric constant with MWCNT content is an indication that these composites could be used as capacitors. It was also found that activation energy related to the ac conductivity decreased with MWCNT concentration. The thermal stability of composites decreased with MWCNT content. The glass transition temperatures of the composites decreased on introduction of MWCNTs.

И З В О Д

ЕЛЕКТРИЧНА И ТЕРМИЧКА СВОЈСТВА КОМПОЗИТА НА БАЗИ КОПОЛИМЕРА БИСФЕНОЛ А-ПРОПОКСИЛАТ-ДИГЛИЦИЛИЛ-ЕТРА И ПИПЕРАЗИНА СА ФУНКЦИОНАЛИЗОВАНИМ MWCNT

SERPIL YILMAZ, MUSTAFA ERSIN PEKDEMIR и MEHMET COŞKUN

University of Fırat, Faculty of Science, Department of Chemistry, 23119 Elazığ, Turkey

У овом раду је приказано формирање композита на бази бисфенол А-пропоксилат-диглицидил-етра и пиперазина у присуству функционализованих вишеслојних карбонских нанотуба (MWCNT; оксидисани MWCNT + аминовани MWCNT). Структура синтетисаних нанокомпозита је потврђена помоћу FTIR и NMR спектроскопије. Нанокомпозити су испитивани у погледу електричних и термичких својстава. Морфологија површина композита је анализирана на основу SEM фотографија. Уочено је да се смањује термичка стабилност и повећава електрична проводљивост у наизменичном електричном пољу и диелектрична константа (релативна пермитивност) са повећањем садржаја (2, 5, 10 и 15 мас. %) функционализованих MWCNT у нанокомпозитима. Електрична проводљивост нанокомпозита се повећавала са порастом температуре, а такође је одређена и дискутована енергија активације електричне проводљивости нанокомпозита.

(Примљено 14. септембра 2017, ревидирано 14. јуна, прихваћено 18. јуна 2018)

REFERENCES

1. S. Iijima, *Nature* **354** (1991) 56
2. A. Bachtold, P. Hadley, T. Nakanishi, C. Dekker, *Science* **294** (2001) 1317
3. H. Ago, K. Petritsch, M. S. P. Shaffer, A. H. Windle, R. H. Friend, *Adv. Mater.* **11** (1999) 1281
4. A. Y. Kasumov, R. Deblock, M. Kociak, B. Reulet, H. Bouchiat, I. Khodos, Y. B. Gorbatov, V. T. Volkov, C. Journet, O. Stephan, M. Burghard, C. R. Acad, *Science* **284** (1999) 1508
5. R. H. Baughman, C. Cui, A. A. Zakhidov, Z. Iqbal, J. N. Barisci, G. M. Spinks, G. G. Wallace, A. Mozzoldi, D. De Rossi, A. G. Rinzler, O. Jaschinski, S. Roth, M. Kertesz, *Science* **284** (1999) 1340
6. C. Niu, E. K. Sichel, R. Hoch, D. Moy, H. Tennet, *Appl. Phys. Lett.* **70** (1997) 1480
7. P. M. Ajayan, S. Iijima, *Nature* **361** (1993) 333
8. X. L. Xie, Y. W. Mai, X. Ping, *Mater Sci. Eng. Rep.* **49** (2005) 89
9. R. Andrews, M. C. Weisenberger, *Curr. Opin. Solid State Mater. Sci.* **8** (2004) 31
10. A. Kausar, I. Rafique, B. Muhammad, *Polym.-Plast. Technol. Eng.* **55** (2016) 1167
11. X. L. Xie, Y. W. Mai, X. P. Zhou, *Mater. Sci. Eng., R.* **49** (2005) 89
12. F. Yakuphanoğlu, I. S. Yahia, G. Barim, B. F. Senkal, *Synth. Met.* **160** (2010) 1718
13. N. G. Sahoo, S. Rana, J. W. Cho, L. Li, S. H. Chan, *Prog. Polym. Sci.* **35** (2010) 837
14. Y. Liu, S. Kumar, *ACS Appl. Mater. Interfaces* **6** (2014) 6069
15. R. Chavan, U. Desai, P. Mhatre, R. Chinchole, *Int. J. Pharm. Sci. Rev. Res.* **13** (2012) 125
16. C. C. Teng, C. C. M. Ma, S. Y. Yang, K. C. Chiou, T. M. Lee, C. L. Chiang, *J. Appl. Polym. Sci.* **123** (2012) 888
17. J. Ma, X. Nan, J. Liu, *Polym. Adv. Technol.* **28** (2017) 166
18. M. M. Rahman, M. Hosur, S. Zainuddin, K. C. Jajam, H. V. Tippur, S. Jeelani, *Polym. Test.* **31** (2012) 1083
19. S. A. Curran, J. Talla, S. Dias, D. Zhang, D. Carroll, D. Birx, *J. Appl. Phys.* **105** (2009) 073711
20. J. H. Lee, J. Kathi, K. Y. Rhee, J. H. Lee, *Polym. Eng. Sci.* **50** (2010) 1433
21. J. Kathi, K. Y. Rhee, *J. Mater. Sci.* **43** (2008) 33
22. H. C. Silvis, J. E. White, US 5, 275, 853 (1994)
23. M. Coşkun, P. Seven, *React. Funct. Polym.* **7** (2011) 395
24. H. Kong, C. Gao, D. Yan, *Macromolecules* **37** (2004) 4022
25. H. H. So, J. W. Cho, N. G. Sahoo, *Eur. Polym. J.* **43** (2007) 3750
26. H. Naceur, A. Megriche, M. E. Maaoui, *Orient. J. Chem.* **29** (2013) 937
27. D. Jaaoh, C. Putson, N. Muensit, *Compos. Sci. Technol.* **122** (2016) 97
28. G. Thenmozhi, J. Santhir, *Int. J. Sci. Res.* **3** (2014) 378
29. G. C. Psarras, E. Manolakaki, G. M. Tsangaris, *Composites, Part A* **34** (2003) 1187
30. K. Abazine, H. Anakiou, M. E. Hasnaoui, M. P. F. Graca, M. A. Fonseca, L. C. Costa, M. E. Achour, A. Oueriagli, *J. Compos. Mater.* **50** (2016) 3283
31. M. Trihotri, U. K. Dwivedi, F. H. Khan, M. M. Malik, M. S. Qureshi, *J. Non-Cryst. Solids* **421** (2015) 1
32. M. S. Lakshmi, B. Narmadha, B. S. R. Reddy, *Polym. Degrad. Stab.* **93** (2008) 201
33. T. Xie, I. A. Rousseau, *Polymer* **50** (2009) 1852.